PCCP

Accepted Manuscript

This is an *Accepted Manuscript*, which has been through the Royal Society of Chemistry peer review process and has been accepted for publication.

Accepted Manuscripts are published online shortly after acceptance, before technical editing, formatting and proof reading. Using this free service, authors can make their results available to the community, in citable form, before we publish the edited article. We will replace this *Accepted Manuscript* with the edited and formatted *Advance Article* as soon as it is available.

You can find more information about *Accepted Manuscripts* in the **Information for Authors**.

Please note that technical editing may introduce minor changes to the text and/or graphics, which may alter content. The journal's standard **Terms & Conditions** and the **Ethical guidelines** still apply. In no event shall the Royal Society of Chemistry be held responsible for any errors or omissions in this *Accepted Manuscript* or any consequences arising from the use of any information it contains.

ARTICLE TYPE

Femtosecond mid-infrared study of the dynamics of water in aqueous sugar solutions[†]

C.C.M. Groot,* and H.J. Bakker

We study the effect of the sugars glucose, trehalose and sorbitol on the reorientation dynamics of water molecules, using polarization-resolved femtosecond infrared spectroscopy. We find that at all sugar concentrations the water dynamics can be described by a single reorientation time constant. With increasing carbohydrate concentration, the water reorientation time constant increases from 2.5 picoseconds to a value of about 15 picoseconds. The slowing down of the water dynamics is strongest for trehalose, followed by glucose and sorbitol.

1 Introduction

Sugars are an important class of biological molecules. In living organisms, they fulfill a wide range of functions, serving for example as energy source or signaling group (when part of a glycoprotein or glycolipid), or acting as a stabilizing osmolyte of proteins under environmental stress conditions[1,2]. Even though this latter property is widely used in industry and biochemistry labs, the exact mechanism by which sugars stabilize proteins against unfolding is still not fully understood[1–3].

Since sugars are preferentially excluded from protein surfaces[1,2], it has been hypothesized that they protect proteins indirectly by modifying the properties of the water solvent. For this reason, people have extensively investigated the properties of water in solutions of sugars, using a wide range of techniques. With Raman spectroscopy[4–6], neutron scattering[6], neutron diffraction[7–9] and THz absorption experiments[10,11], it was found that the water structure around sugars is changed in comparison to the structure of neat water. However, the observed structural changes tend to be quite small[9]. A more pronounced effect is found with techniques that probe the dynamics of the water molecules. Dielectric relaxation[12], NMR[13], time-resolved fluorescence[14] and dynamic light scattering[15,16] studies all show that the dynamics of water slows down significantly near sugar molecules. A similar slowing down effect is seen with molecular dynamics simulations[4,17–19]. However, the different studies do not agree on the magnitude and the spatial extent of the effects of sugar molecules on the dynamics of water. For trehalose

for example, which is the sugar with the highest degree of bioprotectability, different techniques give different results. With NMR measurements of the spin relaxation rate of water ^{17}O in dilute trehalose solutions a modest retardation factor of 1.6 was found, assuming that the hydration shell consists of 47 water molecules[13]. In dynamic light scattering measurements[15] a much larger retardation factor of 5 to 6 was found, for a hydration shell consisting of 25 water molecules. Finally, time-dependent fluorescence Stokes shift measurements of a small THz probe covalently attached to trehalose[14], indicate that trehalose affects the dynamics of more than 150 surrounding water molecules.

Here we report on the effect of different sugars and sugar alcohols on water reorientation dynamics, using polarization-resolved femtosecond infrared spectroscopy. This technique has the advantage that it directly measures the picosecond reorientation dynamics of both water and solute. We studied solutions of glucose, trehalose and sorbitol, as these are all commonly used as stabilizing osmolytes. In addition, glucose is the main monosaccharide unit and energy source in biological systems. Trehalose, on the other hand, is known to be the most bioprotective sugar[3]. Finally, sorbitol is interesting because it is a linear form of glucose; unlike glucose and trehalose it does not contain a pyranose ring, and therefore the comparison between glucose and sorbitol gives information on the effects of sugar conformation on the water reorientation dynamics.

2 Methods

We investigate solutions of glucose, trehalose and sorbitol in isotopically diluted water, using polarization-resolved femtosecond infrared spectroscopy. The solutions are prepared by mixing the carbohydrate (purity >98%, Sigma-Aldrich) with ultrapure milli-Q grade H_2O and D_2O (99.9%D, Cambridge

FOM Institute AMOLF, Science Park 104, 1098 XG, Amsterdam, the Netherlands. Tel: +31 (0)20 754 7100 ; E-mail: cgroot@amolf.nl

Isotope Laboratories) such that the percentage of deuterated hydroxyl groups in the sample is always 4%. After mixing, we stir and heat the solutions to about 50°C to promote dissolution. Upon cooling back to room temperature, the carbohydrates stay well dissolved.

We excite and probe the OD stretch vibrations centered at 2500 cm^{-1}. A short pump pulse, in resonance with the OD vibration at 2500 cm^{-1}, efficiently excites the OD stretch vibrations in the sample, which we then follow by monitoring the absorption of a weaker probe pulse at a variable delay time t. The transient absorption setup is described in ref.[20]. At early delay times, the probe absorption is decreased around 2500 cm^{-1}, due to ground state depletion and $v = 1 \rightarrow 0$ stimulated emission. The absorption is increased around 2300 cm^{-1}, due to $v = 1 \rightarrow 2$ excited state absorption. Both absorption changes decay with the lifetime of the OD stretch vibration. In addition there is a small ingrowing signal associated with sample heating.

By comparing the transient absorption for probe pulses polarized either parallel or perpendicular with respect to the pump polarization, we can determine the reorientation rate of the excited OD oscillators. This determination relies on the fact that OD vibrations aligned parallel to the pump polarization are most efficiently excited. Therefore the parallel transient absorption signal is initially higher than the perpendicular signal. At longer delay times this difference decays to zero due to molecular reorientation. From the parallel ($\Delta\alpha_\parallel$) and perpendicular ($\Delta\alpha_\perp$) transient absorption signals we can construct the isotropic signal:

$$\Delta\alpha_{iso}(\nu,t) = \tfrac{1}{3}(\Delta\alpha_\parallel(\nu,t) + 2\Delta\alpha_\perp(\nu,t)) \qquad (1)$$

Here ν is the frequency and t is the pump-probe delay time. $\Delta\alpha_{iso}$ decays with the lifetime of the vibration and is independent of molecular reorientation. In addition we can construct the anisotropic signal

$$R(\nu,t) = \frac{\Delta\alpha_\parallel(\nu,t) - \Delta\alpha_\perp(\nu,t)}{\Delta\alpha_\parallel(\nu,t) + 2\Delta\alpha_\perp(\nu,t)} \qquad (2)$$

The anisotropic signal is directly proportional to the second order reorientational correlation function, and decays with the rate of molecular reorientation, after a small librational contribution at delay times smaller than 0.5 picoseconds.

To calculate the anisotropic signal associated with the OD stretch vibrations, the parallel and perpendicular absorption signals first have to be corrected for the isotropic heating contribution. As the energy of the excited OD vibrations is ultimately transferred into heat, the relaxation eventually gives rise to a delayed transient absorption signal with the shape of a thermal difference spectrum. To correct for the heating effect, we need to determine the dynamics of this effect with great accuracy. We determine these dynamics in an independent experiment in which we probe the red wing of the OH stretch
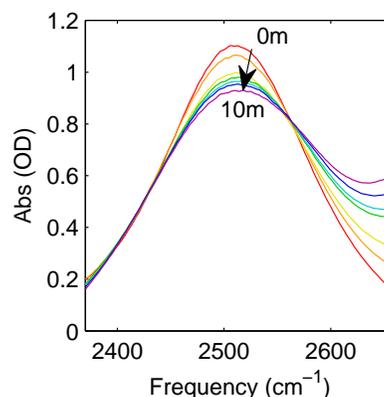
Fig. 1 Linear spectra of aqueous glucose solutions (0,1,2,3,5,7,10 mol/kg), with 4%D:H. Spectra are corrected for H_2O background.

vibration of the H_2O solvent (that is centered at 3400 cm^{-1}) in the spectral region between 2800 and 3100 cm^{-1}.[21] The OH stretch vibration is not directly excited by the 2500 cm^{-1} pump pulse, but its frequency and cross-section are affected by the heating effect that follows the relaxation of the excited OD stretch vibrations. Therefore, the red wing of the OH stretch spectrum forms an excellent reporter of the dynamics of the ingrowing heating effect. With the thus determined heating dynamics, we can correct the transient absorption signals at all delay times for the heating contribution.

3 Results and discussion

3.1 Linear spectra

Figure 1 presents linear spectra of solutions of glucose in isotopically diluted water. The spectra show a broad absorption band centered at 2500 cm^{-1} due to the OD stretch vibrations of water and glucose. With increasing glucose concentration, the center frequency and spectral shape show little change. The absorption around 2500 cm^{-1} slightly decreases, due to the decrease of the concentration of OD oscillators, and the absorption at frequencies above 2600 cm^{-1} increases, due to the absorption of the CH stretch vibrations of glucose. The same trends are observed for solutions of trehalose and sorbitol in isotopically diluted water.

3.2 Isotropic and anisotropic signals

In figure 2 we present isotropic transient absorption signals measured for solutions of trehalose after exciting the sample with a pump pulse at 2500 cm^{-1}. Figure 2a presents the isotropic absorption signal between 2400 and 2600 cm^{-1} for a solution of 3.5 molal trehalose. At early delay times, we observe a bleach at the fundamental transition of the OD stretch
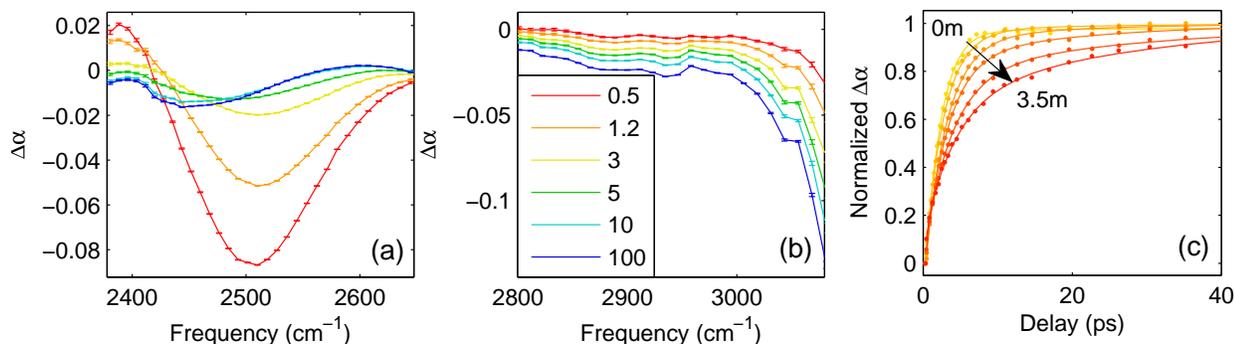
Fig. 2 Isotropic absorption change for solutions of trehalose in water at different picosecond delay times after excitation with a 2500 cm^{-1} pump pulse. a: Absorption change between 2400 and 2600 cm^{-1} (OD stretch vibration) for 3.5 molal trehalose. b: Absorption change between 2800 and 3100 cm^{-1} (tail of OH stretch vibration, heating signal) for 3.5 molal trehalose. c: Absorption change between 2800 and 3100 cm^{-1}, normalized at 100 picoseconds, for different concentrations of trehalose (0, 0.5, 1, 1.5, 2.5 and 3.5 molal). The dotted lines represent empirical triple-exponential fits.

vibration around 2500 cm^{-1}, and an induced absorption at frequencies below 2420 cm^{-1}. At later delay times, these signals have decayed and the transient spectral response is formed by the thermal difference spectrum. Figure 2b presents the isotropic absorption signal between 2800 and 3100 cm^{-1} for the same solution. The bleaching signal (negative absorption change) slowly rises with increasing delay time. This signal is due to the shift and decrease in cross-section of the OH stretch vibrations with temperature, and directly represents the rise in sample temperature. The dynamics of the heat signal between 2800 and 3100 cm^{-1} (normalized at 100 picoseconds) for different concentrations of trehalose are shown in figure 2c. With increasing concentration of trehalose, the heat dynamics slow down considerably. For solutions of glucose and sorbitol we observe a similar slowing down of the heating dynamics with increasing solute concentration.

Figure 3 presents the isotropic transient absorption signals for water and the three studied sugars, after correcting for the heating contribution. All isotropic spectra show a strong bleaching signal around 2500 cm^{-1} due to the bleaching of the fundamental $v = 0 \rightarrow 1$ transition (ground-state bleaching and stimulated emission) and an induced absorption at frequencies below 2420 cm^{-1} due to $v = 1 \rightarrow 2$ excited-state absorption. The spectral shapes are very similar for the different carbohydrates, even at high concentrations, in accordance with the linear spectra. For neat water, we find that the transient absorption changes decay with a frequency-independent time constant of 1.7 picoseconds, in agreement with earlier reports[22]. This time constant represents the vibrational lifetime of the OD stretch vibration of HDO dissolved in D_2O.

The vibrational decay becomes quite inhomogeneous upon the addition of sugar: on the red side of the OD absorption band the decay speeds up compared to neat water, while on the
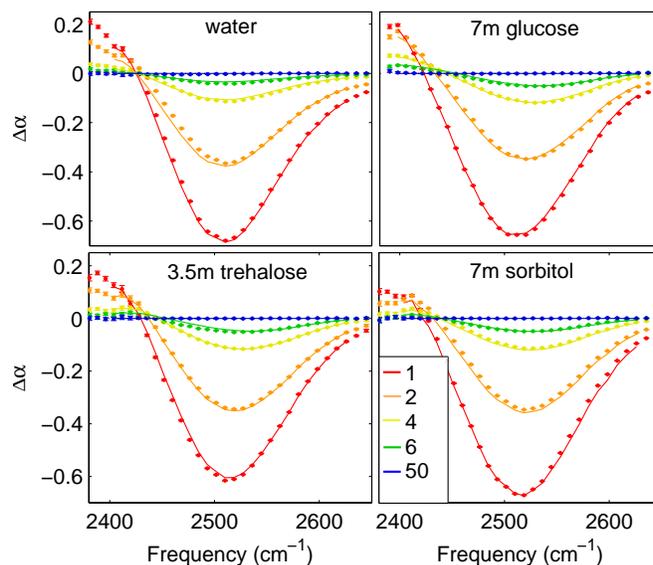
Fig. 3 Isotropic absorption signals for solutions of glucose, trehalose and sorbitol in isotopically diluted water, at five different picosecond delay times after the excitation. The concentrations are given in molal (mol/kg). The solid lines represent fits using the model described in the text.
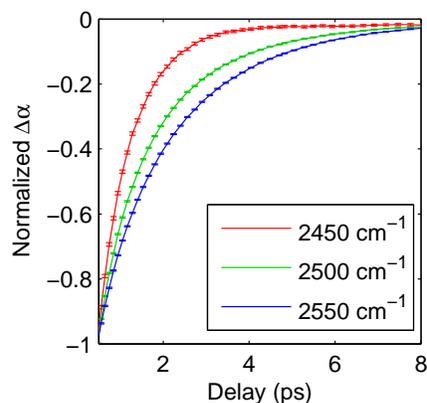
Fig. 4 Isotropic absorption signal for a solution of 3.5 molal trehalose in water, shown for different probe frequencies as a function of delay time (normalized at 0.5 picoseconds).
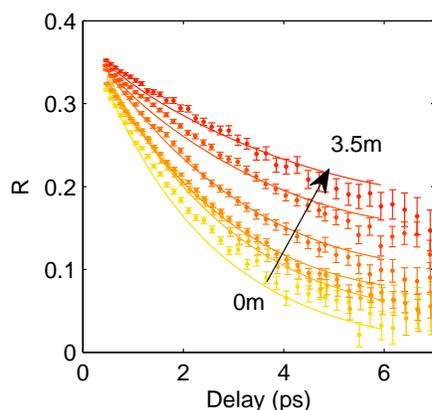
Fig. 5 Anisotropic absorption signal at 2500 cm^{-1} for solutions of trehalose in water of different concentrations (0, 0.5, 1, 1.5, 2.5 and 3.5 molal). Solid lines are description with our model fit.

Fig. 6 a: The isotropic absorption change and b: the anisotropic absorption change as a function of frequency for 0.3 molal 10% deuterated trehalose in DMSO (solid lines are description with model fit). c: Spectral components contributing to isotropic signal (relative amplitudes correspond to 1 ps), c: Anisotropy of the two spectral components as a function of delay time.

blue side of the OD absorption band the decay slows down in comparison with neat water. This observation is further illustrated in figure 4, which shows the isotropic absorption change measured for a solution of 3.5 molal trehalose as a function of delay time at different probe frequencies. The inhomogeneity of the relaxation increases with increasing sugar concentration. This inhomogeneity follows from the fact that both water and sugar contain hydroxyl groups that contribute to the transient spectral response. The frequency-dependent decay of the isotropic spectra shows that the spectral responses and lifetimes of the water and sugar hydroxyl groups differ.

Figure 5 presents the anisotropy of the vibrational excitation (as defined by eq. 2) measured at 2500 cm^{-1} for different concentrations of trehalose. With increasing concentration of trehalose, the decay of the anisotropy strongly slows down. A

similar effect is observed for solutions of glucose and sorbitol. For neat water the anisotropy decays with a timescale of 2.5 ps, in agreement with earlier reports[22].

3.3 Reference measurements in DMSO

The transient absorption signals as shown in figure 3, 4 and 5 contain contributions from both water and sugar hydroxyl groups. To extract the water reorientation dynamics, we need to separate these contributions. To this purpose we performed reference measurements on solutions of the studied sugars in dimethylsulfoxide (DMSO)[20]. The carbohydrates will form similar hydrogen bonds with DMSO as with water, but since DMSO itself does not contain hydroxyl groups, the transient absorption signals only represent the response from the OD stretch vibrations of the sugars. Figure 6 presents the isotropic and anisotropic signals of a solution of 0.3 molal trehalose (10% deuterated) in DMSO. The decay of the isotropic absorption change is again observed to be frequency dependent: on the red side the decay is much faster than on the blue side of the OD absorption band. We find that the dynamics of the isotropic and anisotropic signals can be very well described with two spectral bands, with vibrational relaxation time constants of 1.5±0.2 picoseconds and 5.7±0.2 picoseconds (figure 6c), and different associated anisotropy dynamics

(figure 6d). The responses of glucose and sorbitol dissolved in DMSO can also be very well described with two spectral bands with different vibrational lifetimes and different associated anisotropy dynamics†.

3.4 Spectral decomposition model

Based on the findings for the sugar solutions in DMSO, we analyze the results measured for the sugar solutions in water with a model that includes two spectral bands for the sugar response and one spectral band for the water response. In this model we assume that the relative amplitudes of the sugar and water bands are only defined by the sugar concentration. We further assume that the spectral shape and lifetime of each band do not change with concentration, and fix the spectral shape and lifetime of the water band to the corresponding values for neat water (4% D_2O:H_2O). Each spectral band is assumed to show an associated anisotropy decay of the form:

$$R_i(t) = A_i e^{-t/\tau_i} + B_i \tag{3}$$

The anisotropy dynamics of the two sugar bands are taken to be the same at all concentrations. Only the anisotropy decay of the water band is allowed to vary with concentration. We fit this model to the isotropic absorption and anisotropy signals at all measured concentrations for each sugar. The fit is performed with a single fitting routine that adds the least-square errors for each concentration. During each iteration of the fit, the isotropic absorption signal is spectrally decomposed in three spectra $\sigma_i(\nu)$ for a given set of mono-exponentially decaying populations $N_i(t)$. The error is then determined by comparing the isotropic transient spectral response at all frequencies and delay times to the result of the spectral decomposition $\sum_i N_i(t)\sigma_i(\nu)$. The error for the anisotropic signal is determined by comparing each model anisotropy component R_j (given by A_j, B_j and τ_j) to the following quantity

$$\frac{\frac{1}{3}(\alpha_\parallel - \alpha_\perp) - \sum_{i \neq j} R_i N_i \sigma_i}{N_j \sigma_j} \tag{4}$$

Here $\alpha_\parallel$ and $\alpha_\perp$ are the measured parallel and perpendicular transient spectra, respectively. Equation (4) is based on the following expression:

$$\frac{1}{3}(\alpha_\parallel - \alpha_\perp) = \sum_i R_i N_i \sigma_i \tag{5}$$

The result of the fits are displayed with solid lines in figure 3 and 5. The fits are in good agreement with the data for all sugars†. The spectral band shapes resulting from the fits are shown in the left column of figure 7. For all three sugars, the two bands originating from the sugar hydroxyl groups are red-shifted and blue-shifted with respect to the water band, and have lifetimes around 0.4 ps and 3.8 ps respectively. The
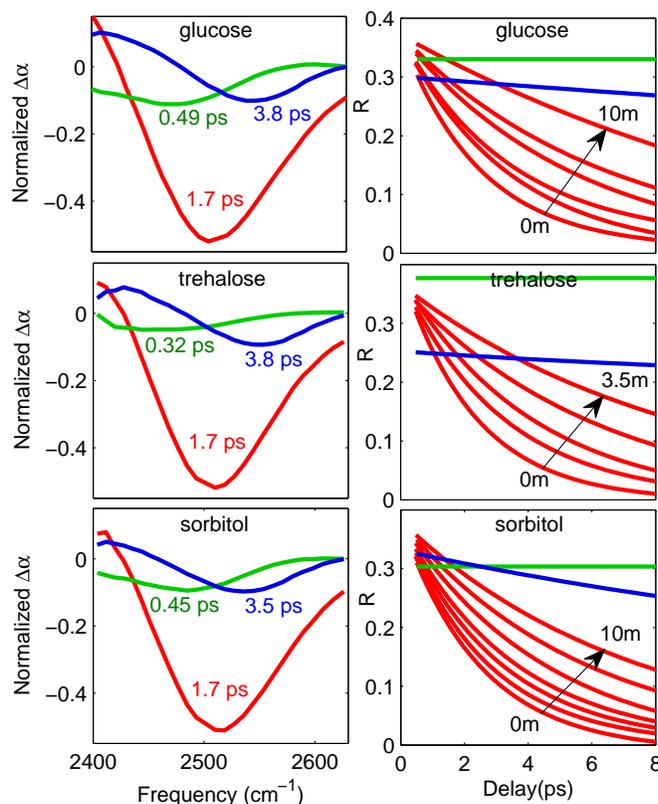
Fig. 7 a: Spectral components of the transient spectral response of aqueous sugar solutions. The spectral components decay with different vibrational lifetimes (indicated as legends). The three panels present the amplitudes of the spectral components at 1 ps after the excitation for the same sugar concentrations that are shown in figure 3). b: Anisotropy as a function of delay time for the two sugar hydroxyl bands (green and blue) and the water hydroxyl band (red), at different sugar concentrations
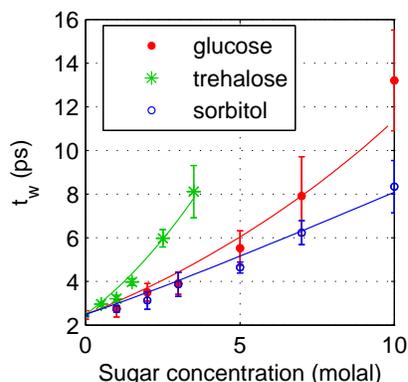
Fig. 8 Water reorientation time constant as a function of sugar concentration. Solid lines represent the description with overlapping hydration shell model described in the text.

band shapes are very similar to what is found for the sugars in DMSO. For sorbitol the center frequencies of the two sugar hydroxyl bands are slightly closer together than for glucose and trehalose.

The anisotropy dynamics of the three spectral bands are shown in the right column of figure 7. It is seen that the anisotropy of the two sugar hydroxyl bands decays very slowly. The anisotropy dynamics of the water hydroxyl band are faster, but strongly slow down with increasing sugar concentration. We find that the final value of the anisotropy (coefficient B in eq. 3) of the water band stays within ±0.015 for all sugars at all concentrations. Hence, the anisotropy decay of the water band can be well characterized by a single reorientation time constant τ_w of which the value depends on the nature of the sugar and its concentration. This reorientation time constant is presented in figure 8 for each sugar as a function of concentration.

3.5 Modeling water reorientation of sugar hydration shells

We measure the reorientation dynamics of water in sugar solutions up to very high concentrations. At the highest concentrations, only 5 to 6 water molecules (and 15 in the case of trehalose) are available per sugar molecule. As a result, the hydration shells of the sugar molecules will overlap which implies that the reorientation dynamics of the water molecules will be affected by the nearby presence of multiple sugar molecules. It is to be expected that the reorientation dynamics of water will be become slower when the number of nearby sugar molecules increases. To account for this effect, we calculate the probabilities that a water molecule is located in zero, one, two or more sugar hydration shells. We assume the sugars to be randomly distributed, which is a reasonable assump-

tion according to neutron diffraction experiments[7,8] and MD simulations[8,23]. The water molecules are largely randomly distributed as well, except for the fact that we define a maximum number of shells to which a water molecule can belong. The distribution depends on the sugar molar concentration (calculated from the sugar molal concentration c_m with $C_M = c_m \cdot \rho / (1000 + c_m \cdot M_{sugar})$) and the size of the hydration shell. The calculation of the distribution of probabilities of the number of hydration shells to which a water molecule belongs is described in detail in the appendix. To translate this distribution to the dynamics of water, we assign increasingly slow reorientation rates to water in zero, one, or two hydration shells. A single retardation factor x relates the reorientation rates, such that the rate decreases a factor x when going from zero to one hydration shell, and x^2 when going from one to two hydration shells. In addition we define the number of water molecules dynamically perturbed by each carbohydrate, i.e. the size of the hydration shell. This model yields a triple exponential anisotropy decay at each sugar concentration that we can approximate well with a single time constant (in the interval of 0-8 picoseconds) to allow for a comparison with the time constant coming from the experiment at the same sugar concentration. Only two parameters, the retardation factor and the hydration shell size, are varied until the calculated water reorientation time constant is in accordance with the experimentally determined values, shown in figure 8. The calculated values are shown as solid lines in the same figure. We find an optimal retardation factor of 1.65±0.15, independently of the type of sugar, and hydration numbers of 24±3, 46±5 and 22±3 for glucose, trehalose and sorbitol, respectively.

4 Discussion

4.1 Solute dynamics

For all investigated sugar solutions, the nonlinear vibrational response of the hydroxyl vibrations can be well described with three spectral bands, each with its own vibrational relaxation time constant and associated anisotropy decay. The two bands associated with the sugar hydroxyl groups probably do not represent two distinct species of sugar hydroxyl groups but rather a continuous distribution of vibrational relaxation time constants across the inhomogeneously broadened sugar hydroxyl absorption band. The vibrational lifetime is observed to be significantly shorter in the red wing than in the blue wing of the absorption band. This is a quite general observation[24–26] that follows from the fact that both the hydroxyl stretch frequency and the vibrational lifetime decrease with increasing strength of the hydrogen bond donated by the hydroxyl group. The shape and vibrational lifetime of the sugar hydroxyl bands are very similar for glucose, trehalose and sorbitol. For sorbitol the two bands are slightly closer in fre-

quency, which suggests that for sorbitol, the relaxation of the OD stretch vibrations is less inhomogeneous than for glucose and trehalose. This might be due to the lower chemical heterogeneity and the greater flexibility of the sorbitol molecule [23] compared to trehalose and glucose.

For all sugars, the anisotropy of the vibrational excitation of the hydroxyl stretch vibrations decays only partially within the experimental time window of <10 ps. The partial decay indicates that the reorientation of the sugar hydroxyl groups occurs within a finite cone angle. The complete decay of the anisotropy requires the molecular reorientation of the entire sugar molecule, which takes tens of picoseconds [13,15]. The sugar hydroxyl band at lower frequencies (green band in figure 7) has a higher and more persistent anisotropy value than the band at higher frequencies. This difference can be explained from the fact that the band at lower frequencies corresponds to more strongly hydrogen bonded hydroxyl groups for which the cone angle will be smaller. The anisotropy decay of the sugar bands is not very different for sorbitol compared to glucose and trehalose, which indicates that the flexibility of the backbone of the sugar does not play a role for the hydroxyl reorientation dynamics occurring on a 10 ps time scale. The reorientation on this time scale is thus only governed by the strength of the local hydrogen-bond interaction.

4.2 Water dynamics

For all three sugars we observe a superlinear increase of the water reorientation time with sugar concentration. Based on our modeling of the water reorientation in the sugar hydration shells, we explain this superlinear behavior from a combination of two effects. The first is that the probability for a water molecule to belong to two or more hydration shells strongly increases with concentration. The second is that the reorientation of water molecules belonging to two or more hydration shells is slower than for water molecules belonging to a single hydration shell. In an NMR study of a solution of trehalose in water a similar superlinear increase of the reorientation time with concentration has been observed [13]. This observation was interpreted as the result of water molecules interacting with multiple trehalose molecules, in agreement with our interpretation. A similar trend has been observed with dielectric relaxation (DR) measurements of solutions of glucose in water [12]. In the NMR and the dielectric relaxation measurements the water dynamics are observed to slow down even more strongly with increasing concentration than in our measurements. A possible explanation may be that the NMR and dielectric relaxation results are more sensitive to collective effects on the spin relaxation and the polarization response, whereas the femtosecond infrared experiments probe the reorientation of single hydroxyl groups.

We find that we can describe the increase in average water
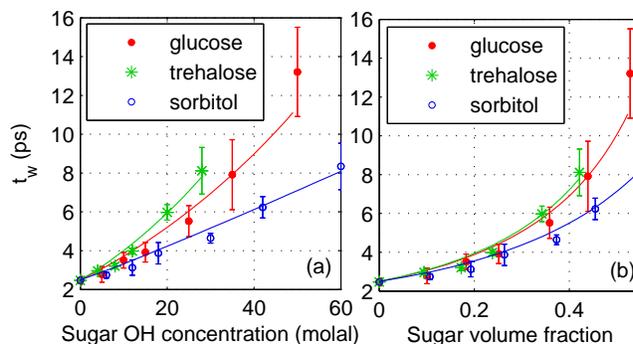
Fig. 9 Water reorientation time constant as a function of a: concentration of sugar hydroxyl groups, b: Sugar volume fraction.

reorientation time with a model that assigns increasingly slow reorientation times to water molecules in zero, one or two carbohydrate hydration shells. From the model we extract a retardation factor of 1.65 ± 0.15. This retardation factor implies that water molecules that are located within the hydration shell of one sugar molecule reorient 1.65 ± 0.15 times slower compared to water molecules in bulk water, while water molecules within the hydration shell of two sugar molecules reorient 2.7 ± 0.3 times slower again. Obviously, this discrete description of the water reorientation in the vicinity of sugars is an approximation of the actual, more diffuse, water reorientation, but it nonetheless indicates the magnitude and extent of the effect of sugars on the water dynamics in concentrated sugar solutions. Interestingly, the retardation we find does not vary significantly with the type of sugar. A similar observation was made using dynamic light scattering measurements [15].

For all investigated sugar solutions the water reorientation can be characterized with a single reorientation time constant. This time constant increases strongly with increasing sugar concentration, reflecting an overall slowing down of the water reorientation. In contrast to the water dynamics around small amphiphilic molecules [27,28] and salts [24,25], we do not observe a clear distinction between bulk-like water and hydration water. For these solutions, it was found that the reorientation of a fraction of the water molecules is strongly retarded, while the remaining water molecules were observed to reorient with the same time constant as observed for neat water, even at high solute concentrations. For the sugar solutions we do not observe such a bimodal distribution of the reorientation time of the water molecules. This finding indicates that the hydration layer in which the water dynamics are affected is far more diffuse around carbohydrates than around ions or hydrophobic molecular groups. The effect on the dynamics of water thus appears to be longer ranged for sugars than for ions or hydrophobic molecular groups.

The long-range character of sugar molecules on the dynam-

ics of water may find its origin in their large number of hydrophilic hydroxyl groups. These hydroxyl groups will form strong hydrogen bonds with nearby water molecules[17], and thus it has been proposed that the effect of sugars on the dynamics of water scales with the number of hydrogen bonds between the sugar and water[11], or alternatively, with the number of sugar hydroxyl groups[15]. Following this idea, we plotted the water reorientation time constant against the number of sugar hydroxyl groups in figure 9a. It is apparent from the figure that the water reorientation time constants we measure do not follow the suggested scaling behavior. Trehalose has a comparatively strong effect on the water dynamics per hydroxyl group, while the effect of sorbitol is relatively weak. This is most apparent at sugar concentrations above 1 molal (trehalose) and 2 molal (glucose, sorbitol).

At higher concentrations, the effect of the overlapping hydration shells becomes important. In this regime the water dynamics are not only influenced by the hydrogen-bond interactions between the sugar molecules and water, but also by the volume that is left for water in between the sugar solutes. In this limit the volume occupied by the sugar solutes starts to play a role. The molecular weight and volume taken by trehalose are almost 2 times as large as for glucose. If we plot the water reorientation time against the sugar volume fraction, as determined from density measurements (figure 9b), we find that the water reorientation time constants in solutions of glucose and trehalose follow almost the same trend up to the highest concentrations.

For sorbitol the effect on the water dynamics is lower than for glucose and trehalose. In modeling the effect of sorbitol on the reorientation, we found that the hydration shell of sorbitol is somewhat smaller than for glucose, in spite of the fact that the molecular masses are nearly the same and sorbitol has 6 hydroxyl groups instead of 5. However, the molecular structure of sorbitol strongly differs from that of glucose and trehalose. The linear flexible structure of sorbitol allows for the formation of intramolecular hydrogen bonds, thus reducing the effect on the surrounding water molecules[23]. The less strong effect of sorbitol on the water reorientation dynamics compared to glucose and trehalose thus likely finds its origin in their difference in molecular structure. For sugar molecules of similar structure like glucose and trehalose, the effect appears to scale quite well with the molecular volume, and surprisingly, less well with the number of hydroxyl groups. These findings suggest that the influence of sugars on the dynamics of the surrounding water involves collective structural effects in which the shape and size of the sugar molecule play important roles.

The long-range effects of sugars on the dynamics of water may in turn play a role in their influence on the conformation of proteins. Experiments show that trehalose is the most effective in preserving biomolecules, compared to other sugars,

and most notably for concentrations above 1 M.[3] This is the concentration range for which we observe a larger effect of trehalose on the water dynamics compared to glucose and sorbitol. The present results are therefore in line with an indirect protection mechanism of sugars via the water solvent.

5 Conclusions

We have investigated the molecular reorientation dynamics of water molecules in aqueous solutions of glucose, trehalose and sorbitol using polarization-resolved femtosecond infrared spectroscopy. With increasing sugar concentration, the decay of the OD stretch vibration becomes more inhomogeneous, due to an increasing contribution of sugar hydroxyl groups. We separate the contributions of sugar and water hydroxyl groups to the nonlinear vibrational signals using a spectral decomposition model. This allows us to observe the dynamics of water and sugar separately.

We find that the sugar hydroxyl groups only move in a restricted cone angle on the timescale of our experiment. The water reorientation is faster, but strongly slows down with increasing sugar concentration. Interestingly, the water reorientation can be characterized with a single reorientation time constant. We find that the water reorientation time τ_w increases from 2.5 ± 0.3 to 13 ± 2 ps for a solution with a glucose concentration of 10 molal, to 8 ± 1 ps for a solution with a trehalose concentration of 3.5 molal, and to 8 ± 1 ps for a solution with a sorbitol concentration of 10 molal. The fact that we do not observe a bimodal distribution of the reorientation time of the water molecules, as for aqueous solutions of small amphiphiles and salts, indicates that the hydration layer of sugars is more diffuse and extents over a longer range.

For all three sugars, the water reorientation time increases superlinearly with sugar concentration. We explain this superlinear dependence with the effect of overlapping hydration shells, and describe the water reorientation time with a model that assigns increasingly slower reorientation times to water molecules in zero, one, two or three carbohydrate hydration shells. From the model, we find that for all three studied sugars the retardation factor is 1.65 ± 0.15. From the model we also find that the hydration shells of glucose, trehalose and sorbitol comprise approximately 24 ± 3, 46 ± 5, and 21 ± 3 water molecules respectively. A comparison of the effects of the different sugars, suggests that the influence of sugars on the dynamics of the surrounding water involves collective structural effects in which the shape and size of the sugar molecule play important roles.

6 Acknowledgements

References

1 T. Arakawa and S. N. Timasheff, *Biochemistry*, 1982, **21**, 6536–6544.

2 G. Xie and S. N. Timasheff, *Biophysical Chemistry*, 1997, **64**, 25 – 43.

3 D. Corradini, E. G. Strekalova, H. E. Stanley and P. Gallo, *SCIENTIFIC REPORTS*, 2013, **3**, 1218.

4 A. Lerbret, F. Affouard, P. Bordat, A. Hédoux, Y. Guinet and M. Descamps, *Journal of Non-Crystalline Solids*, 2011, **357**, 695 – 699.

5 M. E. Gallina, P. Sassi, M. Paolantoni, A. Morresi and R. S. Cataliotti, *The Journal of Physical Chemistry B*, 2006, **110**, 8856–8864.

6 C. Branca, S. Magazù, G. Maisano, S. M. Bennington and B. Fåk, *The Journal of Physical Chemistry B*, 2003, **107**, 1444–1451.

7 J. J. Towey and L. Dougan, *The Journal of Physical Chemistry B*, 2012, **116**, 1633–1641.

8 P. E. Mason, G. W. Neilson, J. E. Enderby, M.-L. Saboungi and J. W. Brady, *The Journal of Physical Chemistry B*, 2005, **109**, 13104–13111.

9 S. E. Pagnotta, S. E. McLain, A. K. Soper, F. Bruni and M. A. Ricci, *The Journal of Physical Chemistry B*, 2010, **114**, 4904–4908.

10 U. Heugen, G. Schwaab, E. Bründermann, M. Heyden, X. Yu, D. M. Leitner and M. Havenith, *Proceedings of the National Academy of Sciences*, 2006, **103**, 12301–12306.

11 M. Heyden, E. Bründermann, U. Heugen, G. Niehues, D. M. Leitner and M. Havenith, *Journal of the American Chemical Society*, 2008, **130**, 5773–5779.

12 K. Fuchs and U. Kaatze, *The Journal of Physical Chemistry B*, 2001, **105**, 2036–2042.

13 L. R. Winther, J. Qvist and B. Halle, *The Journal of Physical Chemistry B*, 2012, **116**, 9196–9207.

14 M. Sajadi, F. Berndt, C. Richter, M. Gerecke, R. Mahrwald and N. P. Ernsting, *The Journal of Physical Chemistry Letters*, 2014, **5**, 1845–1849.

15 L. Lupi, L. Comez, M. Paolantoni, S. Perticaroli, P. Sassi, A. Morresi, B. M. Ladanyi and D. Fioretto, *The Journal of Physical Chemistry B*, 2012, **116**, 14760–14767.

16 D. Fioretto, L. Comez, M. Gallina, A. Morresi, L. Palmieri, M. Paolantoni, P. Sassi and F. Scarponi, *Chemical Physics Letters*, 2007, **441**, 232 – 236.

17 S. L. Lee, P. G. Debenedetti and J. R. Errington, *The Journal of Chemical Physics*, 2005, **122**, 204511.

18 A. Magno and P. Gallo, *The Journal of Physical Chemistry Letters*, 2011, **2**, 977–982.

19 A. Vila Verde and R. K. Campen, *The Journal of Physical Chemistry B*, 2011, **115**, 7069–7084.

20 C. C. M. Groot and H. J. Bakker, *The Journal of Chemical Physics*, 2014, **140**, 234503.

21 S. T. van der Post and H. J. Bakker, *The Journal of Physical Chemistry B*, 2014, **118**, 8179–8189.

22 Y. L. A. Rezus and H. J. Bakker, *The Journal of Chemical Physics*, 2005, **123**, 114502.

23 A. Lerbret, P. Mason, R. Venable, A. Cesro, M.-L. Saboungi, R. Pastor and J. Brady, *Carbohydrate Research*, 2009, **344**, 2229 – 2235.

24 S. T. van der Post, S. Scheidelaar and H. J. Bakker, *Journal of Molecular Liquids*, 2012, **176**, 22 – 28.

25 S. T. van der Post, K.-J. Tielrooij, J. Hunger, E. H. G. Backus and H. J. Bakker, *Faraday Discuss.*, 2013, **160**, 171–189.

26 J. Hunger, K.-J. Tielrooij, R. Buchner, M. Bonn and H. J. Bakker, *The Journal of Physical Chemistry B*, 2012, **116**, 4783–4795.

27 Y. L. A. Rezus and H. J. Bakker, *Phys. Rev. Lett.*, 2007, **99**, 148301.

28 K.-J. Tielrooij, J. Hunger, R. Buchner, M. Bonn and H. J. Bakker, *Journal of the American Chemical Society*, 2010, **132**, 15671–15678.

7 Appendix

In this appendix we present a model to calculate the probabilities that water molecules belong to 1, 2 3, or even more hydration shells of sugar solute molecules. We consider a system containing N_s solute molecules. For each solute molecule the fully filled solvation shell has a volume fraction x (x does not include the volume of the solute) of the total volume, and thus the total volume fraction of the solvation shells in case the shells would not overlap is equal to $N_s x$. The volume fraction x is given by $x = N_h v_w$, where N_h is the number of water molecules in the hydration shell and v_w is the volume of a water molecule ($0.018/N_a$ liter). N_s is equal to N_a times C_s, the solute molar concentration.

To determine the probabilities that a water molecule belongs to a particular number of hydration shells we consider picking N_s times a volume x out of the total volume of the solution and calculate the probability that a molecule is within at least one of the picked volumes x. We define $a^{(1)} = N_s x$. At every selection a molecule has a chance of x to be chosen, and a chance of $1-x$ not to be chosen. The probability that a molecule is not chosen after choosing N_s times a volume fraction x is equal to $(1-x)^{N_s} = (1-x)^{a^{(1)}/x}$. We arrive at the following probabilities of molecules belonging to 0, 1, 2, 3 solvation shells:

$$P^{(1)}(0) = (1-x)^{N_s} = (1-x)^{a^{(1)}/x} = e^{-a^{(1)}} \qquad (6)$$

$$P^{(1)}(1) = N_s x (1-x)^{N_s-1} = a^{(1)} e^{-a^{(1)}}$$

$$P^{(1)}(2) = \frac{N_s(N_s-1)}{2} x^2 (1-x)^{N_s-2} = \frac{[a^{(1)}]^2}{2} e^{-a^{(1)}}$$

$$P^{(1)}(3) = \frac{N_s(N_s-1)(N_s-2)}{6} x^3 (1-x)^{N_s-3} = \frac{[a^{(1)}]^3}{6} e^{-a^{(1)}},$$

where we used that $x \to 0$. In general:

$$P^{(j)}(i) = \frac{[a^{(j)}]^i}{i!} e^{-a^{(j)}}, \qquad (7)$$

where we changed the superscript (1) for the more general superscript (j). It should be noted that $a^{(j)} = \sum_{i=0}^{\infty} i P^{(j)}(i)$.

To account for the fact that molecules can only belong to a maximum number of k solvation shells, we redistribute the probabilities of molecules belonging to more than k shells over molecules belonging to less than k shells. This redistribution is performed with a statistical approach, and will again yield non-zero probabilities of molecules belonging to more than k shells. However, the sum of these probabilities will be smaller than in the first calculation. The procedure is repeated until there are only probabilities of molecules belonging to k shells or less. We define an excess volume $a_{ex}^{(j)}$ of $a^{(j)}$ that is contained in molecules belonging to $k+1$ and even more solvation shells. For $j = 1$ the excess volume $a_{ex}^{(1)}$ is given by:

$$a_{ex}^{(1)} = \sum_{i=k+1}^{\infty} (i-k) P^{(1)}(i), \qquad (8)$$

where the term $(i-k)$ is introduced to account for the fact that a molecule belonging to $i > k$ shells has been chosen $i-k$ times too much. The excess volume $a_{ex}^{(j)}$ has to be redistributed over molecules that belong to less than k solvation shells. As we will calculate the final distribution with an iterative procedure, applying several subsequent calculations of the redistribution of excess volumes $a_{ex}^{(j)}$, we define the distribution $P_c^{(j)}(i)$ as the distribution that results after the j'th iteration. Obviously $P_c^{(1)}(i) = P^{(1)}(i)$.

To calculate the probability distribution associated with the redistribution of $a_{ex}^{(j)}$ we account for the fact that only molecules belonging to less than k shells can be selected. Hence, we renormalize $a_{ex}^{(j)}$ to the volume from which molecules can be selected in the next $j+1$ selection round:

$$a^{(j+1)} = \frac{a_{ex}^{(j)}}{\sum_{i=0}^{k-1} P_c^{(j)}(i)} \qquad (9)$$

Substitution of $a^{(j+1)}$ in equation (7) yields the distribution function $P^{(j+1)}(i)$ of the excess volume $a_{ex}^{(j)}$. The division by $\sum_{i=0}^{k-1} P_c^{(j)}(i)$ accounts for the fact that the volume of molecules from which the molecules can be selected in the $(j+1)$'th round corresponds to the molecules that have only been selected $k-1$ or less times after the j'th round. The volume taken by these molecules is smaller than the original volume by a factor $\sum_{i=0}^{k-1} P_c^{(j)}(i)$. This means that the probability that a particular molecule is selected from this volume is larger than in the case that the excess volume $a_{ex}^{(j)}$ could have been redistributed over all molecules. This larger selection probability is expressed in the fact that $a^{(j+1)} > a_{ex}^{(j)}$. The distribution function $P^{(j+1)}(i)$ is used to determine the corrections to the total probability function $P_c^{(j)}(i)$.

Selection of molecules that belong to $P_c^{(j)}(i)$ 1 or more times in the $(j+1)$'th round (i.e. $P^{(j+1)}(l \geq 1)$, with $l = 1, 2, ...$), will lead to a decrease of $P_c(i)$, i.e. of the fraction of molecules belonging to i solvation shells, irrespective of whether these molecules are chosen 1, 2 or more times. On the other hand, $P_c(i)$ will increase if a molecule belonging to $P_c^{(j)}(i-l)$ is selected l times. The probability of selecting a molecule l times from a particular $P_c^{(j)}(i)$ is given by $P^{(j+1)}(l) P_c^{(j)}(i)$. Hence, the redistribution leads to the following expression for the new, corrected fraction $P_c^{(j+1)}(i)$ of molecules belonging to i solvation shells:

$$P_c^{(j+1)}(i) = P_c^{(j)}(i) - P_c^{(j)}(i) \sum_{i=1}^{\infty} P^{(j+1)}(i) + \sum_{l=0}^{l=i-1} P_c^{(j)}(l) P^{(j+1)}(i-l), i \leq k \qquad (10)$$

In case molecules from $P_c^{(j)}(i)$ $(i < k)$ are selected two or more times $(P^{(j+1)}(i \geq 2) \neq 0)$, the redistribution also leads to a non-zero probability of molecules belonging to $i > k$ solvation shells. As the maximum number of solvation shells to which a molecule can belong is defined by k, the probability of belonging to to $i > k$ solvation shells needs to be redistributed over $P_c(i)$ $(i < k)$. This is done in the following manner. First the probability of molecules of belonging to $i > k$ solvation shells is completely attributed to $P_c^{(j+1)}(k)$:

$$P_c^{(j+1)}(k) = P_c^{(j+1)}(k) + \sum_{l=0}^{k-1} P_c^{(j)}(l) \sum_{i=k-l+1}^{\infty} P^{(j+1)}(i) \qquad (11)$$

The excess selections $i > k$ define a new excess volume $a_{ex}^{(j+1)}$ with a magnitude given by:

$$a_{ex}^{(j+1)} = \sum_{l=0}^{k-1} P_c^{(j)}(l) \sum_{i=k-l+1}^{\infty} (i-k+l) P^{(j+1)}(i) \qquad (12)$$

The case of $a_{ex}^{(1)}$, as expressed in equation (8), applies to the case before any selection was made, i.e. to $P_c^0(0) = 1$ and $P_c^0(i > 0) = 0$. The value of $a_{ex}^{(j+1)}$ evaluated with equation (12) is used in the next iteration in the determination of $P_c(i)$ using equation (9) to transfer $a_{ex}^{(j+1)}$ and $P_c^{(j+1)}(i)$ to $a^{(j+2)}$, equation (7) to calculate the normalized distribution function $P^{(j+2)}(i)$, and equation (10) to calculate $P_c^{(j+2)}(i)$. The calculation is repeated until the probability of molecules belonging to $i > k$ solvation shells has become negligibly small $(\sum_i P_c(i > k) \approx 0)$ or until all molecules are at least k times selected, meaning that $\forall P_c(i < k) = 0$.